atmosphere

MDPI

*Article*

# Investigating Nonlinear Dynamics in Atmospheric Aerosols during the Transition from Laminar to Turbulent Flow

**Marius Mihai Cazacu [1,*], Alin Iulian Roșu [2], Razvan Vasile Ababei [3], Adrian Roșu [4], Decebal Vasincu [5], Dragoș Constantin Nica [6], Oana Rusu [7], Andreea Bianca Bruma [8] and Maricel Agop [1,9]**

1 Department of Physics, "Gheorghe Asachi" Technical University of Iasi, 700050 Iasi, Romania; m.agop@yahoo.com
2 Laboratory of Atmospheric Environment and Climate Change, Technical University of Crete, 73100 Chania, Greece; alin.iulian.rosu@gmail.com
3 Laboratory of Astronomy and Astrophysics, Astronomy Observatory, Research Center with Integrated Techniques for Atmospheric Aerosol Investigation in Romania (RECENT Air), "Alexandru Ioan Cuza" University of Iasi, 700490 Iasi, Romania; razvan.ababei@uaic.ro
4 REXDAN Research Infrastructure, Faculty of Sciences and Environment, "Dunarea de Jos" University of Galati, 800008 Galati, Romania; adrian.rosu@ugal.ro
5 Department of Biophysics, Faculty of Dental Medicine, "Grigore T. Popa" University of Medicine and Pharmacy, 700115 Iasi, Romania; decebal.vasincu@umfiasi.ro
6 Department of Geography, Faculty of Geography and Geology, "Alexandru Ioan Cuza" University of Iasi, 700506 Iasi, Romania; dragos.nica@uaic.ro
7 Department of Materials Science, Materials Science and Engineering Faculty, "Gheorghe Asachi" Technical University of Iasi, 700050 Iasi, Romania; oana.rusu@academic.tuiasi.ro
8 Faculty of Physics, "Alexandru Ioan Cuza" University of Iasi, 700506 Iasi, Romania; bianca_andreea_bruma@yahoo.com
9 Academy of Romanian Scientists, 050094 Bucharest, Romania
* Correspondence: cazacumarius@gmail.com

**Abstract:** This paper investigates the nonlinear dynamics of atmospheric aerosols during the transition from laminar to turbulent flows using the framework of Scale Relativity Theory. It is proposed that the transition from multifractal to non-multifractal scales (in the dynamics of the atmospheric aerosols) can be assimilated to the transition between laminar and turbulent states. These transitions are determined by the multifractal diffusion and deposition processes. The methodology used involves the application of the principle of scale covariance, which states that the laws of atmospheric physics remain invariant with respect to spatial and temporal transformations as well as scale transformations. Based on this principle, several conservation laws are constructed. In such context, the conservation law of the density of states associated with the multifractal-non-multifractal scale transition in a one-dimensional case is then considered. The model describes the non-linear behaviour of atmospheric aerosols undergoing diffusion and deposition processes. The theoretical approach was correlated using experimental data from a ceilometer and radar reflectivity factor data.

**Keywords:** nonlinear dynamics; laminar to turbulent flow; remote sensing



**Citation:** Cazacu, M.M.; Roșu, A.I.; Ababei, R.V.; Roșu, A.; Vasincu, D.; Nica, D.C.; Rusu, O.; Bruma, A.B.; Agop, M. Investigating Nonlinear Dynamics in Atmospheric Aerosols during the Transition from Laminar to Turbulent Flow. *Atmosphere* **2024**, *15*, 366. https://doi.org/10.3390/atmos15030366

Academic Editors: Tianyi Fan and Pengfei Yu

Received: 7 February 2024
Revised: 6 March 2024
Accepted: 14 March 2024
Published: 17 March 2024



## 1. Introduction

Atmospheric aerosol has a direct impact on the atmospheric radiative balance and global climate cycles. It also plays an indirect role in determining the microphysical properties of clouds, which affects physical processes in clouds and the formation of atmospheric precipitation. Aerosol is one of the crucial components in the hydrological cycle. We only refer to the interaction of aerosols with water, which is a significant aspect of aerosol physics. Aerosol particles serve as the nucleus of cloud particle formation, and increased concentrations of aerosol particles modify the microphysical, optical, and radiative properties of clouds. On the other hand, clouds and precipitation trap polluting

aerosols, removing them from the atmosphere, a process known as wet aerosol removal, which is important in air pollution studies [1,2].

Despite the importance of aerosols, their influence on global atmospheric processes has not been fully investigated. Describing their impact on climate is always a challenge. Aerosol dynamics are defined by various and complex mathematical models [3,4]. This statement can be supported by several arguments:

(i) The physical-chemical properties of aerosols;
(ii) The interaction processes of aerosols with water present in the three states of aggregation in the atmosphere;
(iii) The interaction processes of solar radiation with aerosols.

In such a framework, since theoretical mathematical models describing atmospheric dynamics involve the use of nonlinear differential equations, analytical solutions are more difficult to obtain (note that analytical solutions are usually correlated, either special symmetries or adequate boundary conditions [3]). Because of the nonlinearities mentioned above, computational methods are usually preferred.

Computational models are commonly used, either in integer or fractional manifold space (the manifolds in which one operates with $n \in N$—order differentials are defined as integer manifolds, while the manifolds in which fractional differentials are operated are called fractional manifold) [5,6]. The description of atmospheric dynamics can be enhanced by using Scale Relativity Theory [7,8], either for mono-fractal or multifractal atmospheric dynamics. In both cases, the dynamics of the structural units of any type of atmosphere, which is considered a complex system, are described by continuous and non-differentiable curves (fractal curves/multifractal curves). More precisely, by using motion curves with a single fractal dimension, only mono-fractal atmospheric dynamics can be specified [9], while by using motion curves that can have several fractal dimensions simultaneously, multifractal atmospheric dynamics can be specified [10,11]. This procedure has resulted in the following:

(i) A β model for the generation and analysis of atmospheric turbulence [12];
(ii) A computational method for the determination of the planetary boundary layer and its properties [13];
(iii) The removal of atmospheric turbulence through laminar channels [14].

Rosu et al. [12] proposed a multifractal model to understand the dynamics of the turbulent atmosphere by reducing it to the standard β model. The authors suggest that the turbulent atmosphere can be considered a complex system, with its structural units supporting dynamics on continuous but non-differentiable multifractal curves. The authors implement the multifractality approach through the theoretical framework of scale relativity theory with arbitrary and constant fractal dimension, using non-differentiable functions. They argue that the atmosphere is a multifractal due to the continuous and non-differentiable curves of atmospheric particles' trajectories. The equations that underpin atmospheric dynamics are expressed using a scale covariant derivative operator to describe the behaviour of these atmospheric entities [8,15,16].

Ice clouds, also known as cirrus clouds, are important for Earth's climate system and atmospheric processes. They are high-altitude clouds made up of ice crystals and are typically found in the upper troposphere and lower stratosphere [17,18].

Accurately modelling ice clouds is crucial in contemporary atmospheric science due to their significant influence on global climate, weather patterns, and radiative forcing, and their connection to various environmental and societal issues [19,20]. Ice clouds have a profound impact on the Earth's energy balance by affecting both incoming solar radiation and outgoing terrestrial radiation. They possess unique radiative properties that regulate the Earth's temperature. Ice crystals reflect incoming sunlight, but they also trap heat emitted by the Earth, contributing to the greenhouse effect [21–23]. Accurate modelling of ice clouds is essential for assessing their role in global warming, climate change, weather forecasting, and air traffic and aviation.

This paper presents an alternative approach to ice cloud dynamics by implementing the previously discussed mechanisms of atmospheric laminar channels [14]. Rosu et al. [12] recently presented a mathematical model that describes the motion of atmospheric entities, considering both differential and non-differential scale resolutions. The model is based on a set of differential equations for the velocity fields, which reflect the interdependent complex mechanisms involved in the motion of atmospheric entities. The concept of multifractalization by Markov-type stochastic processes was introduced by the authors [24]. This involves specific coefficients that are associated with the transitions from multifractal to non-multifractal states. In atmospheric dynamics, two distinct patterns emerge based on stochastic fractalization/multifractalization: monofractal patterns exhibit homogeneous behaviour with a single fractal dimension and consistent scaling across time intervals, and multifractal patterns display non-homogeneous behaviour with multiple fractal dimensions, allowing for the identification of universal patterns in atmospheric dynamics despite apparent differences [8,9,25].

This paper investigates non-linear behaviours in atmospheric aerosol dynamics at the transition between turbulent and laminar flows using the Scale Relativity Theory. The article is structured as follows: The 'Theoretical Model' section presents a mathematical model that defines, by means of differentiable and nondifferentiable spatial-temporal coordinates, both the differentiable and non-differentiable velocities, and specific constants related to transitions from laminar to turbulence in the atmospheric dynamics. In such context, the singularity spectrum characterizes atmospheric dynamics, emphasizing nature of the atmosphere as a complex system. This section presents an analysis of how differential equations can be used to model the behaviour of atmospheric aerosols at different scales, incorporating diffusion processes and deposition mechanisms within turbulent and laminar dynamics. It also discusses the solution of diffusion equations for initial one-dimensional distributions in unbounded media using Fourier integrals. The 'Results' section presents a study that analysed atmospheric dynamics using data on radar reflectivity factor and ceilometer. The theoretical approach was correlated using experimental data from ceilometer and radar reflectivity factor data, which identified laminar channels at specific altitudes and scales. The analysis revealed patterns of ascending and descending laminar channels at different altitudes, providing insights into atmospheric stability and cloud formations. The final section contains the discussions and conclusions.

## 2. Theoretical Model

It is acknowledged, in accordance with references [12–14], that the atmosphere can be represented as a fractal/multi-fractal mathematical object, both structurally and functionally. The dynamics of this object, as described by the Multifractal Theory of Motion [10], is represented by continuous and non-differentiable curves (multifractal curves), which implies the functionality of the scale covariant derivative.

$$\frac{\hat{d}}{dt} = \partial t + \hat{V}^e \partial_e + D^{ie} \partial_i \partial_e, \quad i, e = 1, 2, 3 \tag{1}$$

where we used the following notations:

$$\begin{gathered} \partial_t = \frac{\partial}{\partial t}, \quad \partial_e = \frac{\partial}{\partial x^e}, \quad \partial_i \partial_e = \frac{\partial}{\partial x^i} \frac{\partial}{\partial x^e} \\ \hat{V}^e = V_D^e - i V_F^e, \quad i = \sqrt{-1} \\ D^{ie} = \frac{1}{4} (dt)^{\left[\frac{2}{f(\alpha)}\right]-1} \left( d^{ie} + i \bar{d}^{ie} \right) \\ d^{ie} = \left( \lambda_+^i \lambda_+^e - \lambda_-^i \lambda_-^e \right), \quad \bar{d}^{ie} = \left( \lambda_+^i \lambda_+^e + \lambda_-^i \lambda_-^e \right) \end{gathered} \tag{2}$$

In relations (1) and (2), $x^e$ represents the spatial coordinates, described by continuous and nondifferentiable mathematical functions that depend on scale resolution. The temporal coordinate, $t$, is described by continuous and differentiable mathematical functions that are independent of scale resolution. $V_D^e$ represents the differentiable velocity (i.e., the velocity at differential scale resolution), while $V_F^e$ represents the nondifferentiable velocity

(i.e., the velocity at nondifferentiable scale resolution). $\lambda_+^e$ and $\lambda_-^e$ are specific constants of the differentiable-nondifferentiable scale transition associated with the forward and backward atmospheric dynamics, respectively. The singularity spectrum of order $\alpha$, denoted by $f(\alpha)$, is determined by $\alpha = \alpha(D_F)$, where $D_F$ is the fractal dimension of the motion curves of the structural units of any atmosphere. It is important to note that the atmosphere is always assimilated to a complex system [8,11–14].

In this context, using the singularity spectrum of order $\alpha$ to describe atmospheric dynamics has clear advantages:

i. The dynamics of the structural units of the atmosphere may exhibit a dominant fractal dimension, which could aid in identifying a global atmospheric pattern that is compatible with a certain global atmospheric structurality and functionality.
ii. The dynamics of the structural units of the atmosphere may contain a "set" of fractal dimensions, which could aid in identifying zonal atmospheric patterns that are compatible with specific local atmospheric structures and functions.
iii. Through the $\alpha$-order singularity spectrum, one can identify universality classes in the field of atmospheric dynamics, even when the attractors associated with these dynamics have different aspects.

The explicit form of the tensor $D^{ie}$, i.e., that associated with the non-multifractal scale transition, is dictated by multifractalization through stochasticity. The most common method of fractalization is through stochastic processes [9,10]. In this context, it is important to clarify that the stochastic or chaotic processes used in the study of atmospheric dynamics can be categorized into two types. The first type includes homogeneous atmospheric dynamics, which are characterized by a single global fractal dimension and exhibit the same scaling properties in any time interval (such as fractional Brownian processes). The second category comprises atmospheric dynamics that can be described using multiple fractal dimensions and quantify only local singularities, known as multifractal processes.

Therefore, we can distinguish following types of atmospheric dynamics:

i. Multifractal atmospheric dynamics via Markov stochasticity imposed by the following constraints [7,24]:

$$\lambda_+^i \lambda_+^e = \lambda_-^i \lambda_-^e = -2\lambda\delta^{ie} \tag{3}$$

where $\lambda$ is a diffusion-type coefficient associated with the multifractal-non-multifractal scale transition and $\delta^{ie}$ is the Kronecker pseudotensor. In such an alternative:

$$D^{ie} \to i\lambda(dt)^{\left[\frac{2}{f(\alpha)}\right]-1} \tag{4}$$

so that Equation (1)becomes as follows:

$$\frac{\hat{d}}{dt} = \partial_t + \hat{V}^e\partial_e - i\lambda(dt)^{\left[\frac{2}{f(\alpha)}\right]-1}\partial^e\partial_e \tag{5}$$

ii. Multifractal atmospheric dynamics by non-Markov stochasticity imposed by the following constraints [12,13]:

$$d^{ie} = 4\alpha\delta^{ie}, \ \ \overline{d}^{ie} = -4\beta\delta^{ie} \tag{6}$$

where $\alpha$ and $\beta$ are diffusion-type coefficients associated with the multifractal-non-multifractal scale transition. In such an alternative:

$$D^{ie} = (\alpha - i\beta)(dt)^{\left[\frac{2}{f(\alpha)}\right]-1}, \tag{7}$$

so that Equation (1) becomes the following:

$$\frac{\hat{d}}{dt} = \partial_t + \hat{V}^e\partial_e - (\alpha - i\beta)\ (dt)^{\left[\frac{2}{f(\alpha)}\right]-1}\partial^e\partial_e \tag{8}$$

Assuming now the functionality of the principle of scale covariance, according to which the laws of atmospheric physics remain invariant with respect to both spatial and temporal transformations and scale transformations, different conservation laws can be constructed.

For example, if one applies the complex operator (8) to the density of states $\rho$, then the conservation law takes the following form:

$$\frac{\hat{d}\rho}{dt} = \partial_t \rho + \hat{V}^e \partial_e \rho - (\alpha - i\beta)\ (dt)^{[\frac{2}{f(\alpha)}]-1} \partial^e \partial_e \rho \tag{9}$$

or yet, explained on resolution scales as follows:

$$\partial_t \rho + V_D^e \partial_e \rho + \alpha\ (dt)^{[\frac{2}{f(\alpha)}]-1} \partial^e \partial_e \rho = 0 \tag{10}$$

at differential scale resolutions, i.e., as follows:

$$-V_F^e \partial \rho - \beta\ (dt)^{[\frac{2}{f(\alpha)}]-1} \partial^e \partial_e \rho = 0 \tag{11}$$

at non-differential scale resolutions. Next if we denote with the following:

$$V^e = V_D^e - V_F^e \tag{12}$$

the velocity associated with the multifractal-non-multifractal scale transition, by adding relations (10) and (11), the conservation law of the density of states associated with the multifractal-non-multifractal scale transition is obtained as follows:

$$\partial_t \rho + V^e \partial_e \rho + (\alpha - \beta)\ (dt)^{[\frac{2}{f(\alpha)}]-1} \partial^e \partial_e \rho = 0 \tag{13}$$

In the following, we present the consequences of such a differential equation in modelling atmospheric dynamics. For this purpose, let us consider the differential Equation (13) in the one-dimensional case and subject to the following constraint:

$$V^e \equiv (0, 0, V = const) \tag{14}$$

This becomes the following:

$$\frac{\partial \rho}{\partial t} + V \frac{\partial \rho}{\partial z} - D \frac{\partial^2 \rho}{\partial z^2} = 0 \tag{15}$$

where we made the notation as follows:

$$D = (\beta - \alpha)\ (dt)^{[\frac{2}{f(\alpha)}]-1} \tag{16}$$

where $D$ depends on the aerosols (geometrical and physical properties), atmosphere, and scale resolution scale properties.

The above model can describe, for example, at various scale resolutions, nonlinear behaviours of atmospheric aerosols that obey simultaneously diffusion and deposition processes through transitions from turbulence to laminar dynamics (diffusion and deposition processes are discussed in their classical sense, with no reference to optical processes). From this perspective, the turbulence–laminar transition will work as multifractal–nonmultifractal scale transition where V denotes the deposition rate associated with such transition.

By making the variable change as follows:

$$\rho(z,t) = n(z,t) \exp\left(\frac{Vz}{2D} - \frac{V^2 t}{4D}\right) \tag{17}$$

which implies the following:

$$\begin{aligned} \tfrac{\partial \rho}{\partial t} &= \left(\tfrac{\partial n}{\partial t} - \tfrac{V^2 n}{4D}\right) \exp\left(\tfrac{Vz}{2D} - \tfrac{V^2 t}{4D}\right) \\ \tfrac{\partial \rho}{\partial z} &= \left(\tfrac{\partial n}{\partial z} + \tfrac{Vn}{2D}\right) \exp\left(\tfrac{Vz}{2D} - \tfrac{V^2 t}{4D}\right) \\ \tfrac{\partial^2 \rho}{\partial z^2} &= \left(\tfrac{\partial^2 n}{\partial z^2} + \tfrac{V}{D}\ \tfrac{\partial n}{\partial z} + \tfrac{V^2 n}{4D^2}\right) \exp\left(\tfrac{Vz}{2D} - \tfrac{V^2 t}{4D}\right) \end{aligned} \tag{18}$$

the differential Equation (15) becomes as follows:

$$\frac{\partial n}{\partial t} = D \frac{\partial^2 n}{\partial z^2} \tag{19}$$

From the initial conditions and the boundary one as follows:

$$\begin{gathered}\rho(z,0)=\rho_0=const\\ \rho(0,t)=0\end{gathered} \tag{20}$$

the boundary conditions corresponding to $n$ are obtained, i.e., as follows:

$$\begin{gathered}n(z,0)=n_0\exp\left(\frac{Vz}{2D}\right)\\ n(0,t)=0\end{gathered} \tag{21}$$

This problem can be reduced to one without boundary conditions by extending the solution to include the region $z<0$, where $n$ assumes an initial distribution that simulates the boundary condition for $z=0$ at any time $t>0$. At the same time one can choose the following:

$$n(z,0)=n(-z,0) \tag{22}$$

so that for any extended region, the initial condition will be as follows:

$$n(z,0)=\begin{cases}n_0\exp\left(\frac{Vz}{2D}\right),\ z>0\\ -n_0\exp\left(-\frac{Vz}{2D}\right),\ z<0\end{cases} \tag{23}$$

The problem is how to solve the diffusion equation for an initially specified dimensional distribution in an unbounded medium. This can be solved by developing the solution as a Fourier integral:

$$n(z,t)=\int_{-\infty}^{+\infty}\phi(k,t)\exp(ikz)dk \tag{24}$$

$$\phi(k,t)=\frac{1}{2\pi}\int_{-\infty}^{+\infty}n\left(z',t\right)\exp\left(-ikz'\right)dz' \tag{25}$$

After substituting the differential Equation (19) we obtain the following:

$$\frac{\partial\phi}{\partial t}+k^2D\phi=0 \tag{26}$$

with the solution as follows:

$$\phi(k,t)=\phi(k,0)\exp\left(-k^2Dt\right) \tag{27}$$

where $\phi(k,0)$ was obtained by substituting the initial distribution $n$ into Equation (25). Therefore, Equation (24)can be expressed as an integral over the entire initial distribution as follows:

$$n(z,t)=\frac{1}{2\pi}\int_{-\infty}^{+\infty}\int_{-\infty}^{+\infty}n\left(z',0\right)\exp\left(-k^2Dt\right)\exp\left[ik\left(z-z'\right)\right]dz'dk \tag{28}$$

Once the integral above is resolved with respect to $k$, solving it for $n$ becomes straightforward, leading to the following:

$$n(z,t)=\frac{1}{(4\pi Dt)^{\frac{1}{2}}}\int_{-\infty}^{+\infty}n\left(z',0\right)\exp\left[-\frac{(z-z')^2}{4Dt}\right]dz' \tag{29}$$

The solution can be completed by substituting Equation (23) into Equation (29) and calculating the integral. The result for $\rho(z,t)$ is given by the following equation:

$$\rho(z,t)=\frac{n_0}{2}\exp\left(-\frac{V^zt}{D}\right)+\frac{n_0}{2}\exp\left(-\frac{V^zt}{D}\right)\cdot\left[\frac{erf(z-Vt)}{(4Dt)^{\frac{1}{2}}}+\frac{erf(z+Vt)}{(4Dt)^{\frac{1}{2}}}\right] \tag{30}$$

where $erf(x)$ is the Laplace function given by the following:

$$erf(x)=\frac{1}{2\sqrt{\pi}}\int_0^{\infty}\exp\left(-x^2\right)dx \tag{31}$$

values of this function being tabulated.

In Figure 1, we illustrate the variations in dimensionless coordinates (used here as '*adim*'), namely reduced $z(adim)$ and reduced $t(adim)$, with respect to density dependencies. It is evident that, at a dimensionless rate of $V/D = 0.1$, $\rho$ experiences an initial increase with reduced $z(adim)$ for small values of reduced $t(adim)$ and subsequently decreases. Conversely, for larger reduced $z(adim)$, $\rho$ decreases with reduced $z(adim)$. In the case of a dimensionless rate $V/D = 10$, $\rho$ increases with reduced $z(adim)$ for small, reduced $t(adim)$ values and then stabilizes, remaining constant. Meanwhile, for larger reduced $t(adim)$, $\rho$ remains constant throughout.

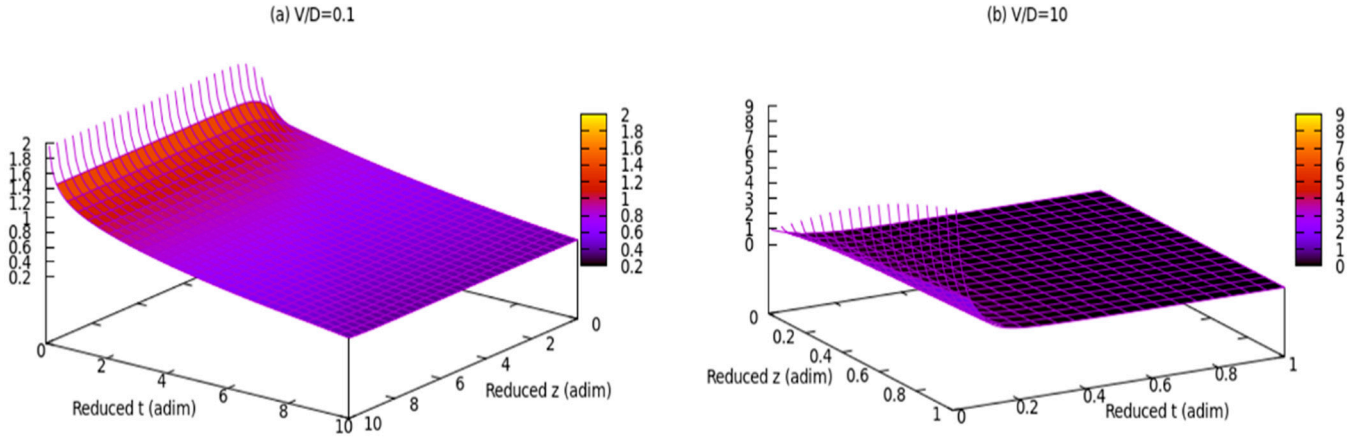


**Figure 1.** A 3D plot of reduced density as a function of reduced *time* and $z$ according to Equation (30).

The deposition rate of the aerosol on the surface, $z = 0$, is given by the following:

$$\begin{aligned} I(t) = -\vec{j}(0,t)\hat{e}_z &= D\left(\frac{\partial n}{\partial t}\right)_{z=0} \\ &= n_0\left\{\frac{V}{2}\cdot\left[1 + erf\left(\frac{V^2 t}{4D}\right)^{\frac{1}{2}} + \left(\frac{D}{n_0 t}\right)^{\frac{1}{2}}\exp\left(-\frac{V^2 t}{4D}\right)\right]\right\} \end{aligned} \tag{32}$$

Figure 2 illustrates a 3D depiction of deposition rate in relation to time and $V^2$. This provides a qualitative depiction of the deposition rate, indicating that an increase in quadratic velocity could result in the highest deposition rate over a shorter time period. However, over an extended period, the deposition rate behaviour may undergo a reversal.

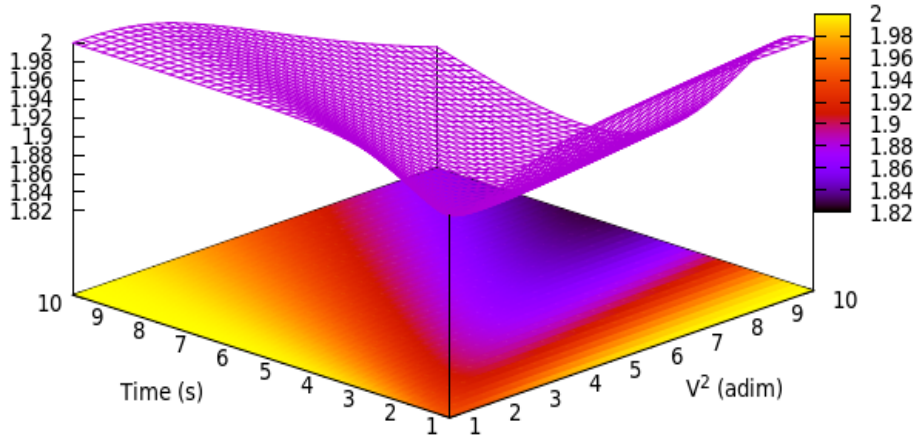


**Figure 2.** A 3D representation of deposition rate indicated by the colour gradient as a function of time and $V^2$ according to Equation (32). $V^2$ and time are reduced coordinates.

Both Figures 1 and 2 show that both density and deposition rate stabilize in space and time. Such a situation is realised at the boundary between turbulent and laminar dynamics, i.e., according to [12,13] along the laminarity channel.

According to Equation (32) the diffusion current is infinite at $t = 0$. This is because an infinite gradient of the concentration has been artificially assumed at $z = 0$, $t = 0$.

For $t \ll t_e = \frac{4D}{V^2}$, Equation (32) becomes the following:

$$\frac{I(t)}{n_0} = \left(\frac{D}{\pi t}\right)^{\frac{1}{2}} + \frac{V}{2} \tag{33}$$

Which is equal to the diffusive deposition speed in the absence of sedimentation plus half the velocity in the case of pure sedimentation. For particles of radius $r = 0.1$ µm and 1 µm into the air, at $p = 10^3$ hPa and $T = 293$ K, $t_e$ is about 40 s, i.e., $4{\cdot}10^{-3}$ s, assuming a density of a particle is 2 g/cm$^3$. For $t \gg t_e$, the deposition speed is $I(t) = n_0 V$ so the Brownian motion has no effect.

In reality, the atmosphere is not motionless, and neither is the Earth's surface a perfect wall. In general, there will be an upward flow of atmospheric aerosols (with respect to aerosol transport in the absence of emission cumulation), usually through turbulent diffusion, which tends to balance sedimentation and other processes at different timescales.

Turbulence in the atmosphere leads to the mixing of air masses and the diffusion of particles, including pollutants, water vapor, and other substances. This turbulent diffusion can be thought of as a mechanism that redistributes matter within the atmosphere, contributing to the upward transport of particles against gravitational settling [26].

## 3. Results

To facilitate the comparison of our theoretical findings with empirical data, we must undertake the computation of laminar data, as outlined in the preceding methods section, using radar reflectivity factor data. Additionally, ceilometer data has been extracted for comparison. In this study, we employed a CHM15k ceilometer operating at a wavelength of 1064 nm and a DJUG RPG-FMCW-94-DP Doppler non-scanning mode cloud radar platform (radar reflectivity factor data) [27]. These instruments are situated at the UGAL–REXDAN research facility in Galați, Romania, located at coordinates 45.435125 N, 28.036792 E, and positioned at an elevation of 65 m above sea level. It is noteworthy that the selection and deployment of these instruments strictly adhere to the standards mandated by the Aerosol Clouds and Trace Gases Research Infrastructure community (ACTRIS) [27]. The ACTRIS Cloudnet data portal (which includes central management, quality assurance, provenance, and storage) provides a service for processing and curating ground-based cloud remote sensing measurements that has been recognized by the scientific community since 2003 [27–30].

For the computational aspects of our analysis, all necessary calculations were executed using Python 3.10.

In the context of atmospheric dynamics, we have employed the agreed methodology proposed by Rosu et al. [12,14] and Cazacu et al. [13]. This methodology utilises Lyapunov exponents in order to identify laminar channels within turbulent flows [12–14]. The Lyapunov exponents are used to identify these regions of laminar behaviour in turbulent atmospheric flows by analysing the rate of divergence or convergence of nearby trajectories in the system [9]. This can help in understanding the complex behaviour of atmospheric flows and potentially lead to the development of more accurate models for predicting and controlling these flows.

The purpose of this approach is to explore the utilization of the application of multifractal and scale-relativistic theory to model atmospheric dynamics, with a goal to identify laminar and non-laminar regions within the intrinsically chaotic and turbulent atmosphere.

The approach used involves the logistic-type approximation of multifractal equations of motion, coupled with simpler gauge models, to identify instances of laminar behaviour within turbulent flows at certain scales. This is based on the understanding that

atmospheric parameters can be modelled as multifractal functions, which undergo scale symmetry breaking at each stage of a turbulent energy cascade. This methodology identifies quasi-laminar behaviour near the planetary boundary layer height and laminar channels throughout an atmospheric column. These findings could enhance our understanding of complex vertical transport behaviours.

One important factor is the correlation between Lyapunov exponents and laminar channels, which can be analysed through bifurcation diagrams and logistic maps [12–14]. By using inequalities related to Lyapunov exponents, it is possible to identify the presence of laminar, periodic, or non-chaotic behaviour at specific scales. This approach utilises the relationship between the logistic map, which is known for its period-doubling behaviour and chaotic regimes, and the equations that govern atmospheric velocity fields, though in an approximate manner.

The experimental data from a ceilometer (lidar) platform and radar reflectivity factor data were used to validate the theoretical approach. Analysis of this data allowed us to identify laminar channels, which indicate quasi-laminar behaviour at certain altitudes and scales.

Figure 3 presents the overall atmospheric time-series characterization obtained from the Cloudnet database [27] using both ceilometer and radar reflectivity factor data. The atmosphere is dominated by large ice cloud particles. It should be noted that, for this application, the ceilometer is generally unsuitable as a data-collecting platform. Additionally, applications related to laminar channels extrapolated in the atmosphere through multifractal theory have only been developed using ceilometer or lidar data so far. The ceilometer is unable to obtain higher altitude data in cloudy conditions due to oversaturation of the backscattered light sensor, as shown in Figure 4. Therefore, it is necessary to use radar reflectivity factor data, as shown in Figure 5. This marks the first instance of radar data being employed for laminar channel applications.

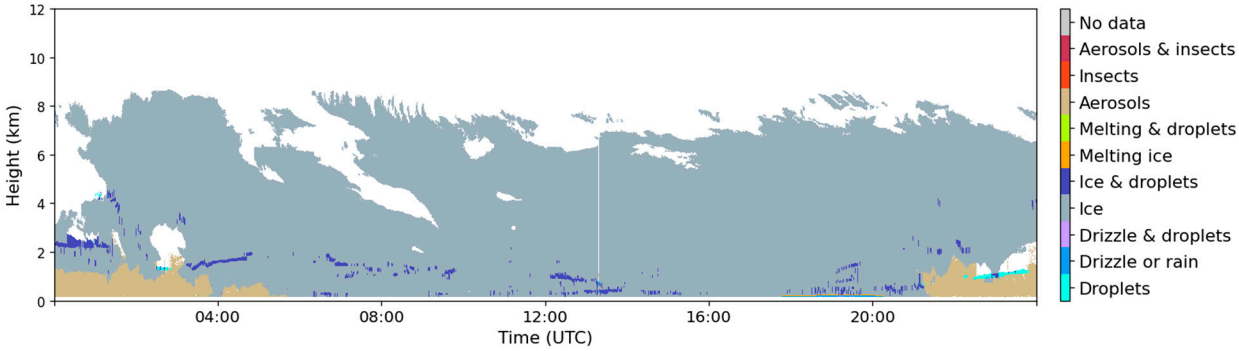


**Figure 3.** Data categorization obtained via radar and ceilometer data, 4 February 2023, Galați, Romania.

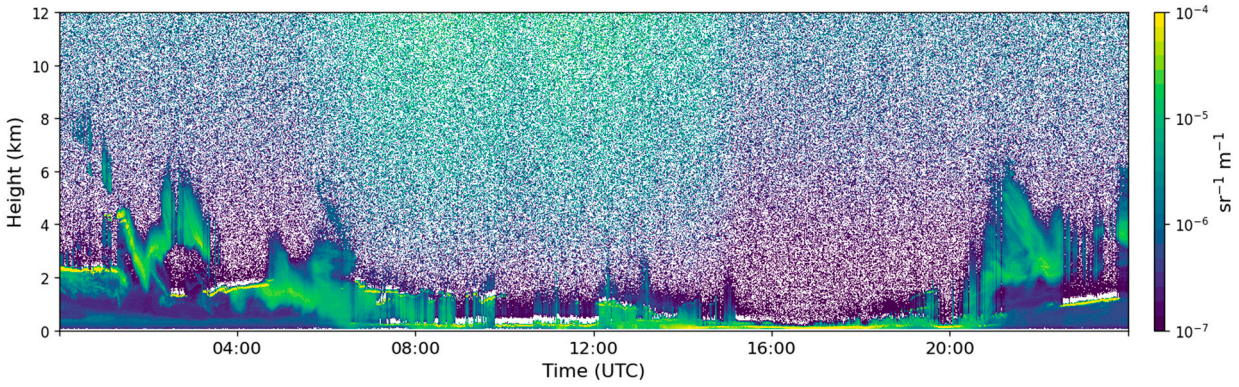


**Figure 4.** Ceilometer data, 4 February 2023, Galați, Romania.

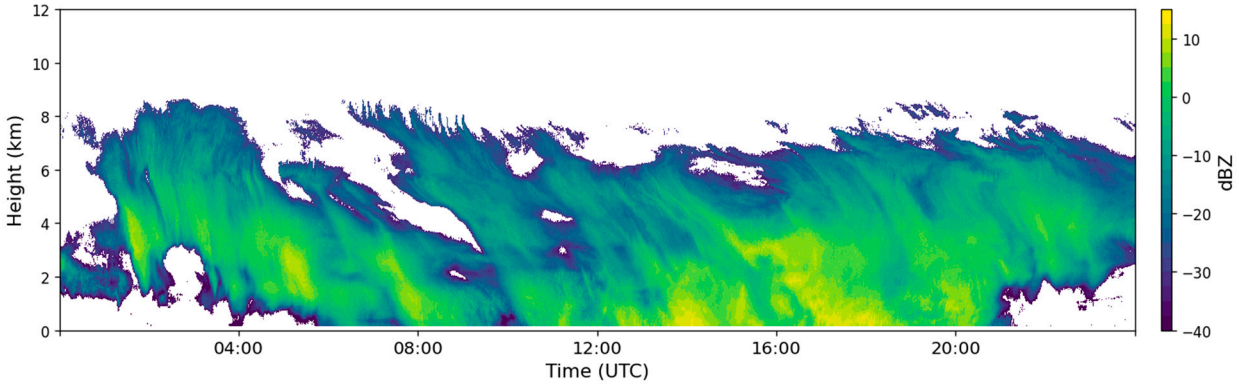


**Figure 5.** Radar reflectivity factor time series, 4 February 2023, Galați, Romania.

Figure 6a accurately describes the descent of cloud formations through lower altitude descending laminar channels. However, it is interesting to note that weak ascending laminar channels are observed at higher altitudes. The explanation is that in this region, the top of the cloud formation does not descend but exits the profile range of the radar reflectivity factor. In other words, that part of the cloud is ascending in a direction that is not accessible to the radar, and thus it appears to be descending. The laminar analysis proves to be useful in differentiating such cases.

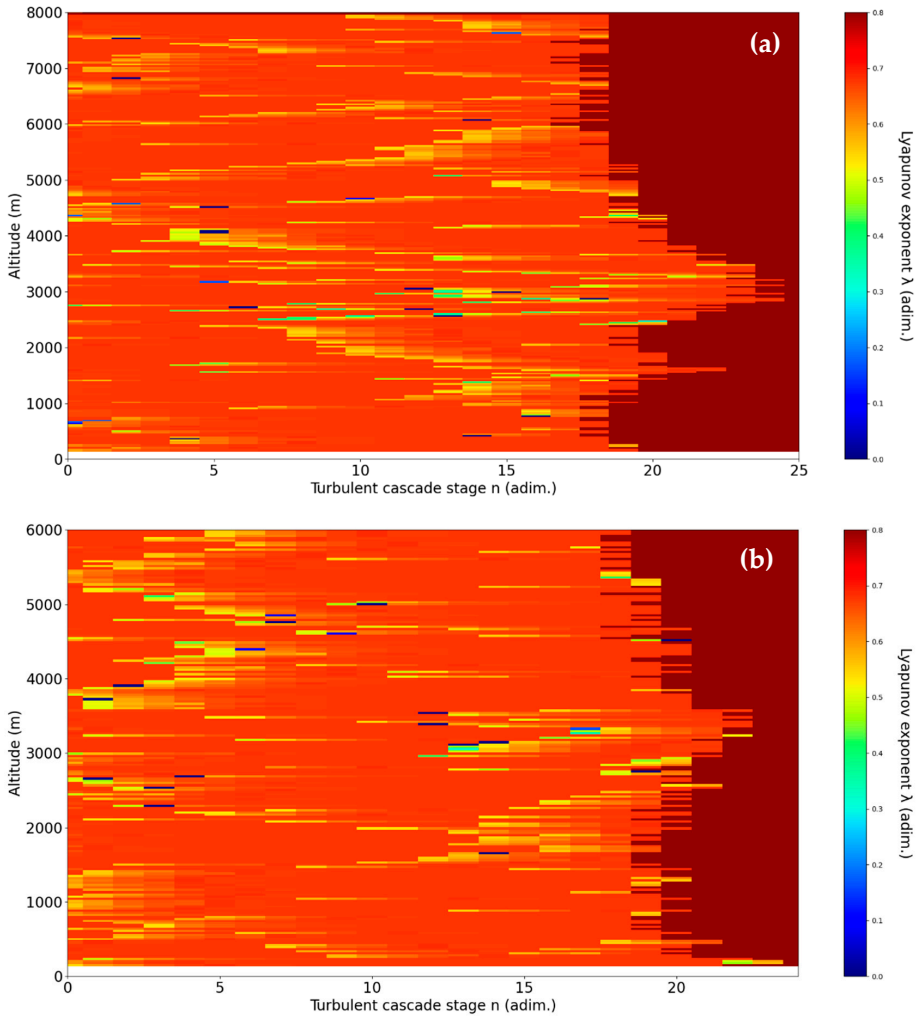


**Figure 6.** *Cont.*

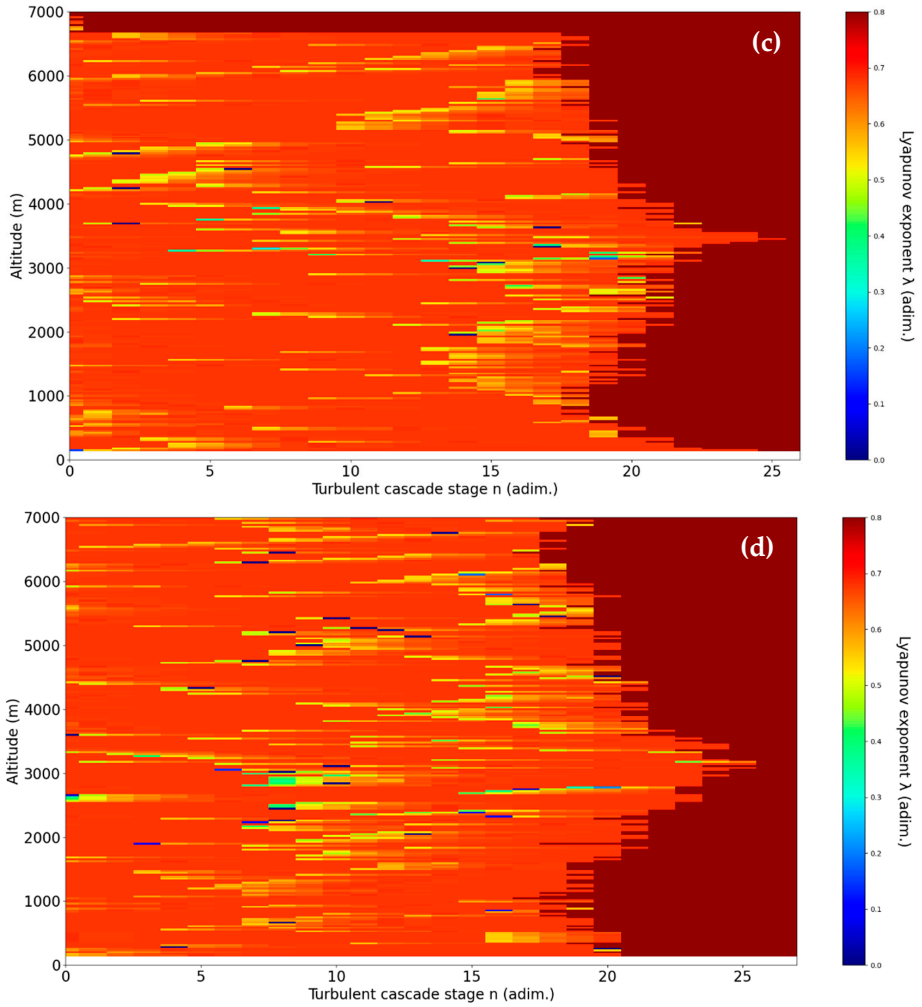


**Figure 6.** Laminar channels profile analysis at different moments of 4 February 2023, Galati, Romania. (**a**) corresponds to 04:00, (**b**) 12:00, (**c**) 16:00, and (**d**) 20:00.

Also, anomalous laminar bands appear in the upper regions, which are representative of the very sudden fluctuations and instabilities which are visible at the top of the cloud in that timeframe in Figure 4. In any case, it seems that the laminar channel analysis can be used to determine when upper parts of cloud masses exhibit high instability.

In Figure 6b, in this particular timeframe, atmospheric stability is mostly expected, and this is what the laminar analysis also shows. There is no significant ascending or descending laminar channels.

In Figure 6c, stability can be seen by the raw data and by the laminar analysis; however, the analysis shows ascending laminar channels at higher altitudes. It is visible, however, that the cloud formation is indeed slightly ascending at higher altitudes in this instance, and thus the laminar analysis correctly predicts atmospheric behaviour. Once again, in the instance analysed in Figure 6d, we are expecting stability, and stability is indeed found. Another interesting pattern is noticed in the analysis, and it must be explained: the peak that appears in the turbulent cascade stage axis always appears in areas with the largest number of backscattering bodies. This occurs because high numbers of turbulent cascade stages indicate areas of very low dissipation, and thus, in such areas, cloud formations are dissipated much slower and airborne ice densities increase. It is then apparent that the laminar analysis can show which areas of the profile have the most airborne ice.

Figures 6a and 7 shows an interesting correlation with our model as they demonstrate a significant gradient of ice particle speed at 4:00 at relatively low height, indicating a laminar channel. This is also suggested by the ceilometer and radar reflectivity data, which

show an increased backscattering profile at similar heights. This is consistent with the previous described theoretical model (see for example Equation (33), in which it is observed that $\frac{V}{2}$ is the velocity associated with the laminar–turbulent flow transition, speed that can be assimilated to the sedimentation rate of aerosols, while $\left(\frac{D}{\pi t}\right)^{\frac{1}{2}}$ corresponds to diffusion deposition speed inversely proportional to $(t)^{-\frac{1}{2}}$ and proportional to $(D)^{\frac{1}{2}}$, coefficient assimilated to fractal–nonfractal transition, i.e., the transition from laminar to turbulent flows), which can predicts an increased deposition rate at the transition from laminar to turbulent flows.

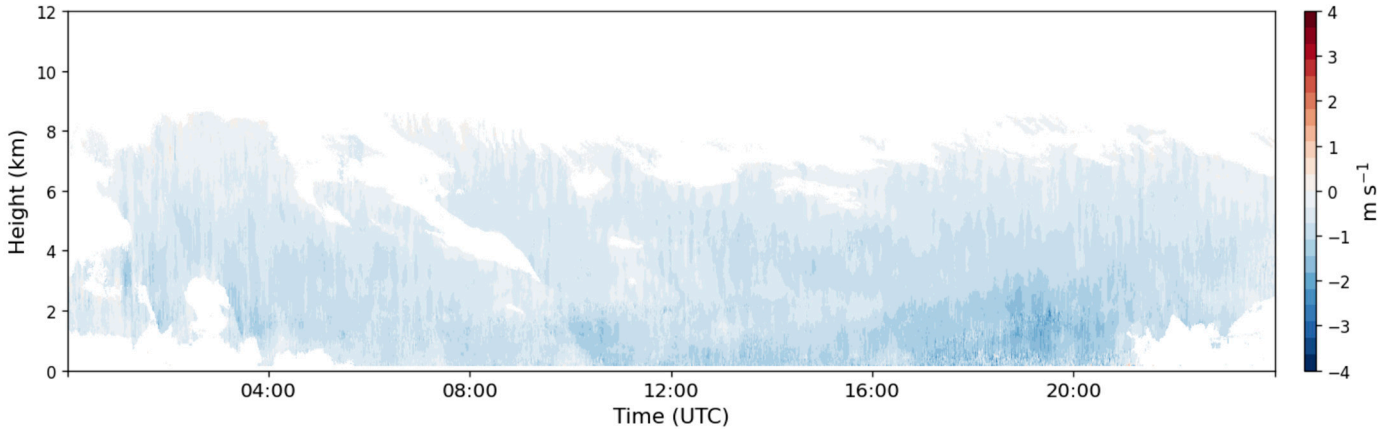


**Figure 7.** The time series of Doppler velocity of 4 February 2023, Galati, Romania.

## 4. Discussions and Conclusions

This paper presents a mathematical model that describes the non-linear behaviour of atmospheric aerosol dynamics during the transition from laminar to turbulence using Scale Relativity Theory. The transition from laminar to turbulence can be associated with a shift from multifractal to non-multifractal scales, and the velocity field associated with this transition acts as a deposition rate. This transition is governed by the multifractal diffusion and deposition processes.

In the context of laminar analysis, it is important to note that complete laminarity is rarely observed when this analysis is applied to radar reflectivity factor data. Instead, quasi-laminarities are mostly observed because a radar platform operates at higher wavelengths, and the backscattering "bodies" are larger. Therefore, at larger scales compared to aerosols alone, laminar flow may not always be present, or it may be present but have a reduced effect on larger bodies such as airborne water in both solid and liquid form. The study found that ceilometers are mostly inappropriate for collecting data in conditions with large ice cloud masses due to oversaturation of the backscattered light sensor. This limitation necessitates the use of radar reflectivity factor data for analysing such atmospheric conditions. For the first time, radar reflectivity factor data has been used to analyse laminar channels in the atmosphere. The use of radar reflectivity factor data was essential in characterizing cloud formations and detecting atmospheric instabilities.

The analysis of the laminar channel was able to distinguish between descending and ascending cloud formations and identify areas of atmospheric instability. The analysis also revealed the presence of quasi-laminarities processes (in accordance with the chaotic dynamics theory [24,25]). This indicates that larger backscattering bodies, such as airborne water in solid and liquid form, do not always exhibit laminarities. The analysis showed that regions with increased airborne ice densities corresponded to areas with a higher number of turbulent cascade stages, indicating lower energy dissipation. This finding suggests that laminar analysis can identify the areas of the atmosphere with the most airborne ice.

**Author Contributions:** Conceptualization, M.A., A.I.R. and M.M.C.; methodology, M.M.C., A.I.R. and R.V.A.; software, A.I.R., R.V.A. and A.B.B.; validation, M.M.C. and M.A.; formal analysis, M.M.C., A.I.R., R.V.A., A.R., D.V., D.C.N., O.R., A.B.B. and M.A.; investigation, M.M.C., A.I.R., R.V.A., A.R., D.V., D.C.N., O.R., A.B.B. and M.A.; resources, M.M.C., A.I.R., R.V.A., A.R., D.V., D.C.N., O.R., A.B.B. and M.A.; data curation, M.M.C., A.I.R., R.V.A. and M.A.; writing—original draft preparation, M.M.C., A.I.R., R.V.A., A.R., D.V., D.C.N., O.R., A.B.B. and M.A.; writing—review and editing, M.M.C., A.I.R., R.V.A. and M.A.; visualization, A.I.R., R.V.A. and A.B.B.; supervision, M.M.C. and M.A.; project administration, M.M.C. and M.A.; funding acquisition, M.M.C., A.I.R., R.V.A., A.R., D.V., D.C.N., O.R., A.B.B. and M.A. All authors have read and agreed to the published version of the manuscript.

**Funding:** This research received no external funding.

**Institutional Review Board Statement:** Not applicable.

**Informed Consent Statement:** Not applicable.

**Data Availability Statement:** The raw data supporting the conclusions of this article are available via Cloudnet at: https://cloudnet.fmi.fi/search/data, accessed on 6 February 2024.

**Acknowledgments:** The authors acknowledge the UGAL–REXDAN cloud remote sensing facility and Cloudnet data availability (https://cloudnet.fmi.fi/site/galati, accessed on 6 March 2024).

**Conflicts of Interest:** The authors declare no conflicts of interest.

## References

1. Colbeck, I.; Lazaridis, M. *Aerosol Science*; Wiley Online Library: West Sussex, UK, 2014.
2. Kulkarni, P.; Baron, P.A.; Willeke, K. *Aerosol Measurement: Principles, Techniques, and Applications*, 3rd ed.; John Wiley & Sons, Inc.: Hoboken, NJ, USA, 2011. [CrossRef]
3. Seigneur, C.; Hudischewskyj, A.B.; Seinfeld, J.H.; Whitby, K.T.; Whitby, E.R.; Brock, J.R.; Barnes, H.M. Simulation of Aerosol Dynamics: A Comparative Review of Mathematical Models. *Aerosol Sci. Technol.* **1986**, *5*, 205–222. [CrossRef]
4. Aloyan, A.E.; Yermakov, A.N.; Arutyunyan, V.O. Modeling the influence of ions on the dynamics of formation of atmospheric aerosol, Izvestiya. *Atmos. Ocean. Phys.* **2021**, *57*, 104–109. [CrossRef]
5. Berselli, L.C. *Three-Dimensional Navier-Stokes Equations for Turbulence*; Academic Press: Cambridge, MA, USA, 2021; pp. 1–313. [CrossRef]
6. Ilhan, E.; Veeresha, P.; Baskonus, H.M. Fractional approach for a mathematical model of atmospheric dynamics of $CO_2$ gas with an efficient method. *Chaos Solitons Fractals* **2021**, *152*, 111347. [CrossRef]
7. Nottale, L. *Scale Relativity and Fractal Space-Time: A New Approach to Unifying Relativity and Quantum Mechanics*; Imperial College Press: London, UK, 2011; pp. 403–425.
8. Dong, Q.; Wang, Y.; Li, P. Multifractal behavior of an air pollutant time series and the relevance to the predictability. *Environ. Pollut.* **2017**, *222*, 444–457. [CrossRef] [PubMed]
9. Cristescu, C.P. Nonlinear Dynamics and Chaos. In *Theoretical Fundaments and Applications*; Romanian Academy Publishing House: Bucharest, Romania, 2008.
10. Agop, M.; Paun, V.P. On the New Perspectives of Fractal Theory. In *Fundaments and Applications*; Romanian Academy Publishing House: Bucharest, Romania, 2017.
11. Fernández-Martínez, M.; Sánchez-Granero, M.A. A new fractal dimension for curves based on fractal structures. *Topol. Its Appl.* **2016**, *203*, 108–124. [CrossRef]
12. Roşu, I.A.; Cazacu, M.M.; Ghenadi, A.S.; Bibire, L.; Agop, M. On a Multifractal Approach of Turbulent Atmosphere Dynamics. *Front. Earth Sci.* **2020**, *8*, 216. [CrossRef]
13. Cazacu, M.M.; Roșu, I.A.; Bibire, L.; Vasincu, D.; Rotundu, A.M.; Agop, M. Theoretical and Experimental Designs of the Planetary Boundary Layer Dynamics through a Multifractal Theory of Motion. *Fractal Fract.* **2022**, *6*, 747. [CrossRef]
14. Roșu, I.A.; Nica, D.C.; Cazacu, M.M.; Agop, M. Cellular Self-Structuring and Turbulent Behaviors in Atmospheric Laminar Channels. *Front. Earth Sci.* **2022**, *9*, 1344. [CrossRef]
15. Benzi, R.; Paladin, G.; Parisi, G.; Vulpiani, A. On the multifractal nature of fully developed turbulence and chaotic systems. *J. Phys. A Math. Gen.* **1984**, *17*, 3521. [CrossRef]
16. Paladin, G.; Vulpiani, A. Anomalous scaling laws in multifractal objects. *Phys. Rep.* **1987**, *156*, 147–225. [CrossRef]
17. Yang, P.; Baum, B.A. Satellites and Satellite Remote Sensing: Remote Sensing: Cloud Properties. In *Encyclopedia of Atmospheric Sciences*, 2nd ed.; Elsevier: Amsterdam, The Netherlands, 2015; pp. 116–127. [CrossRef]
18. Schoeberl, M.R.; Jensen, E.J.; Pfister, L.; Ueyama, R.; Avery, M.; Dessler, A.E. Convective Hydration of the Upper Troposphere and Lower Stratosphere. *J. Geophys. Res. Atmos.* **2018**, *123*, 4583–4593. [CrossRef]
19. Dagan, G.; Yeheskel, N.; Williams, A.I.L. Radiative forcing from aerosol–cloud interactions enhanced by large-scale circulation adjustments. *Nat. Geosci.* **2023**, *16*, 1092–1098. [CrossRef]

20. Yi, B. Diverse cloud radiative effects and global surface temperature simulations induced by different ice cloud optical property parameterizations. *Sci. Rep.* **2022**, *12*, 10539. [CrossRef] [PubMed]
21. Hong, Y.; Liu, G.; Li, J.L.F. Assessing the Radiative Effects of Global Ice Clouds Based on CloudSat and CALIPSO Measurements. *J. Clim.* **2016**, *29*, 7651–7674. [CrossRef]
22. Hang, Y.; L'Ecuyer, T.S.; Henderson, D.S.; Matus, A.V.; Wang, Z. Reassessing the Effect of Cloud Type on Earth's Energy Balance in the Age of Active Spaceborne Observations. Part II: Atmospheric Heating. *J. Clim.* **2019**, *32*, 6219–6236. [CrossRef]
23. Zou, L.; Griessbach, S.; Hoffmann, L.; Spang, R. A global view on stratospheric ice clouds: Assessment of processes related to their occurrence based on satellite observations. *Atmos. Chem. Phys.* **2022**, *22*, 6677–6702. [CrossRef]
24. Mandelbrot, B.B. *Fractal and Chaos*; Springer: Berlin/Heidelberg, Germany, 2004.
25. Jackson, E.A. *Perspectives of Nonlinear Dynamics*; CUP Archive: Cambridge, UK, 1989; Volume 1.
26. Rekier, J.; Chao, B.F.; Chen, J.; Dehant, V.; Rosat, S.; Zhu, P. Earth's Rotation: Observations and Relation to Deep Interior. *Surv. Geophys.* **2021**, *43*, 149–175. [CrossRef]
27. Rosu, A.; Constantin, D.; O'Connor, E.; Voiculescu, M. Categorize Data from Galati on 04 & 05 of February 2023, ACTRIS Cloud Remote Sensing Data Centre Unit (CLU) 2022. Available online: https://cloudnet.fmi.fi/search/visualizations?site=galati&dateFrom=2023-02-05&dateTo=2023-02-05 (accessed on 28 January 2024).
28. Illingworth, A.J.; Hogan, R.J.; O'Connor, E.J.; Bouniol, D.; Brooks, M.E.; Delanoé, J.; Donovan, D.P.; Eastment, J.D.; Gaussiat, N.; Goddard, J.W.F. Cloudnet: Continuous Evaluation of Cloud Profiles in Seven Operational Models Using Ground-based Observations. *Bull. Am. Meteorol. Soc.* **2007**, *88*, 883–898. [CrossRef]
29. Delanoë, J.M.E.; Hogan, R.J. A Variational Scheme for Retrieving Ice Cloud Properties from Combined Radar, Lidar, and Infrared Radiometer. *J. Geophys. Res.* **2008**, *113*. [CrossRef]
30. Cloudnet Data Portal. Publications. Available online: https://cloudnet.fmi.fi/publications (accessed on 6 March 2024).